Unilag Journal of Medicine, Science and Technology (UJMST) Vol 6. No. 1, 2018

WEAR AND CORROSION CHARACTERISTICS OF SILICON CARBIDE SURFACE MODIFIED MILD STEEL

Amuda, M.O.H.[1,*], Lawal, T. F.[2], Daramola, O.[3], Awarun, A. B.[4] and Subair, W. O.[5]
[1-4]Materials Development and Processing Research Group (MADEPREG), Department of Metallurgical and Materials Engineering, University of Lagos, Lagos, Nigeria 101017
[5]Engineering Materials Department, Nigeria Building and Road Research Institute, Km 10, Idiroko-Ota Road, Ogun State
*Corresponding Author: mamuda@unilag.edu.ng

ABSTRACT
The wear and corrosion characteristics of silicon carbide (SiC) modified mild steel surface have been studied. SiC was deposited on mild steel using gas metal arc melting under varying process parameters. Microstructural analysis using optical microscopy indicated the formation of SiC reinforced dendritic structure in the substrate with varying degree of dilution relative to specific process parameter. The improvement obtained in the wear behaviour of the surface modified substrate was attributed to its higher hardness which was influenced by the formation of SiC reinforced dendritic structure in the substrate. Similarly, the corrosion behaviour of the surface modified substrate analyzed using gravimetric analysis and linear polarisation improved across the three media considered. In each of these media, the improvement in corrosion rate peaked at 29%, 33% and 35% in 0.5MHCl, 0.5MNaOH and 0.7MNaCl, respectively, at heat input of about 1.3 kJ/mm. This heat input corresponds to a melting current of 250 A and electrode traverse speed of 5 mm/sec. The improvement obtained in both the wear and corrosion resistances of the surface modified mild steel suggests that low-cost gas metal arc melting technique which is conventionally used for welding can be readily adapted for surface modification as an alternative to the capital intensive laser melting technique.

Keywords: Corrosion Rate, Gas Metal Arc Melting, Silicon Carbide, Surface Modified Mild Steel, Wear Behaviour

1.0 INTRODUCTION

Mild steels present attractive combination of bulk properties that are appropriate for applications in automobile, chemical, agricultural and structural industries (Harish *et al*., 2014). Some of these attributes include excellent ductility, toughness, malleability, tensile strength, weldability and economics. However, in addition to these attributes, materials for the identified industries are equally expected to possess adequate surface characteristics such as excellent wear and corrosion resistances (Majumdar, 2017; Dyuti *et al*., 2011; Majumdar *et al*., 2008). But, these are lacking in mild steel which necessitates the need for additional treatment of the steel in order to optimise its benefits.

Traditional surface treatment techniques for improving surface characteristics in mild steel are based on regulated bulk heat treatment such as temper hardening or

case hardening and induction hardening. A major challenge with these techniques is the incidence of distortion and cracking arising from thermal strain induced in the treated materials due to the differential heating and cooling cycle generated during the process (Edenhofer *et al.*, 2015). Additionally, it is equally difficult to incorporate materials with superior properties such as ceramics or super alloys onto the surface layer of treated materials (Schneider, 2013).

Alternative approaches to improving these properties involves alteration of the near surface region via processes such as thermochemical processes, chemical vapor deposition (CVD), physical vapor deposition (PVD), flame spraying and plasma spraying. These processes either generate mechanical bonding with the surface or generate both mechanical and chemical bonding to derive a diffusion layer with a modified structure and chemical composition (Krastev, 2012). Though, substantial improvement in wear and corrosion resistances have been attributed to these processes, they are, however, not suitable for all alloys particularly mild steel. Therefore, a different approach involving local melting of the substrate's surface with a heat source to form either a ceramic compound or a metal powder incorporated recast layer has been reported in literature with substantial improvement in surface properties (Krastev, 2012). In this approach, the heat source is generated from any of electron beam melting, gas metal arc, plasma transfer arc, laser melting and tungsten inert gas (TIG) torch melting process. The technique of local melting to form a recast layer offers the benefit of high efficiency, relative simplicity and economic use of alloying element. Such technique is characterized with dispensing a regulated quantum of energy, fast heating and cooling rates as well as a very high thermal gradient. It is significant to note that the application of the technique is not limited to specific material, and it confers both generic and specific microstructural and metallurgical advantages on treated materials (Manuwar *et al.*, 2010; Abbas and Ghazanfar, 2005).

Literature documents the application of some of the high energy melting processes in the deposition of hard ceramics especially carbides of Tungsten (WC), Titanium (TC) and Silicon (SiC) to improve the functional surface properties of mild steel (Mohd *et al.*, 2018; Darabara *et al.*, 2012). In this instance, extensive knowledge base is available on the incorporation of SiC on the substrate of mild steel for improved wear behaviour via high energy melting. The widespread use of SiC for surface modification arises from its combination of properties including low density, good electrical and thermal conductivity, high strength and hardness, good oxidation, corrosion and creep resistance at high temperature (Wahab *et al.*, 2006).

Majumdar (2010) reported that the microstructure and mechanical characteristics of laser melted SiC surface modified mild steel is strongly influenced by the processing parameters and surface remelting conditions. It was established that the thickness of the modified zone increases with increasing laser power and decreasing scanning speed. The microstructural constituent of the zone consisted of fine grained ferrite, finely dispersed precipitates of iron silicides and low volume fraction of martensite. The use of shrouding gas coarsened the microstructure and reduced the area fraction of silicide phase. It equally reduced the microhardness and the wear resistance. However, surface remelting in nitrogen atmosphere produced predominantly iron nitrides with few silicon nitrides resulting in increased microhardness and imporved wear resistance. In another work, Grum and žnidaršič (2008) established that the introduction of graphite during re-melting in nitrogen atmosphere promoted the formation of martensite along with silicides of iron which generated a higher microhardness and wear resistance than obtained by Majumdar (2010). Further, Roman *et al*. (2013) reported that mild steel laser surface alloyed with SiC exhibited higher resistance to crack initiation and growth compared to untreated mild steel. Munawar *et al.* (2010) in another instance reported increasing hardness in mild steel substrate modified with SiC and B4C ceramic compounds using electron beam melting. The work equally reported that the lattice parameters of the incorporated ceramic compounds are affected by the electron beam melting.

Laser and electron beam melting techniques though deliver high powder density to substrate with minimal distortion of the substrate; yet, the techniques require both huge capital outlay and technical expertise. Researchers have made attempt to adapt medium range power density processes such as TIG and gas metal arc (GMA) melting processes for surface modification (Quintino, 2014). Muñoz *et al.* (2016) incorporated SiC in the substrate of mild steel using TIG torch melting process and reported that the microstructure and mechanical properties of the modified substrate are influenced by energy density, shielding gas, particle size, distribution and the volume fraction of the incorporated SiC ceramic compound. The work established that the width of the substrate remelted zone increases with corresponding increase in hardness and wear resistance in relation to the particle size, volume fraction and distribution of SiC. The microstructure in this instance consists primarily of dendrites and a eutectic mixture of M_7C_3 carbides and austenite. Literature is rich on the adoption of TIG torch melting process for surface modification but such is not available for GMA melting technique. GMA technique like TIG torch melting generates its heat source from an electric arc between the electrode and the base metal. But unlike TIG torch melting, it uses a

consumable electrode, requires less technical expertise and is more affordable (Weman, 2012; Lathabai, 2011). Other than these, it is free from safety concern unlike the other fusion melting processes (Mazumder, (2017).

In spite of the attractive characteristics of the GMA technique, there is virtually no information in the literature on the adaption of the process for the surface modification of mild steel. Accordingly, the present study sought to investigate the wear and corrosion characteristics of SiC surface modified mild steel produced using GMA melting technique. The study equally investigated the influence of process parameters on the surface topography, degree of dilution and microstructure of the substrate modified layer. Corrosion characteristic was evaluated using both gravimetric and polarization techniques.

2.0 MATERIALS AND METHODS

The 5 mm thick mild steel sheet with spectra composition presented in Table 1 was sectioned into 100 x 100 mm test samples. The sectioned samples were cleaned and degreased in a solution of benzene to remove grease. The cleaned substrate was then surface roughened with emery paper. This was done to facilitate mechanical interlocking between the substrate surfaces and the ceramic coating material.

Table 1: Chemical composition of mild steel substrate

Materials	**Elemental Composition (wt. %)**					
	C	**Si**	**Mn**	**S**	**P**	**Fe**
Mild Steel Substrate	0.17	0.40	0.79	0.04	0.040	98.56

SiC powder of 99.9% purity and average particle size of 45 micron was used for the study. The powder was formed into a pasty mass by dissolving in a solution of poly vinyl alcohol (PVA) as described in Daramola (2016) and Awarun (2017). The mass was evenly spread on the substrate and the pre-coated substrate was dried at room temperature followed by oven drying at 60^{o}C for 24 hours to remove moisture. The image of the substrate materials in its various stages through the powder preplacement stage is shown in Fig. 1.

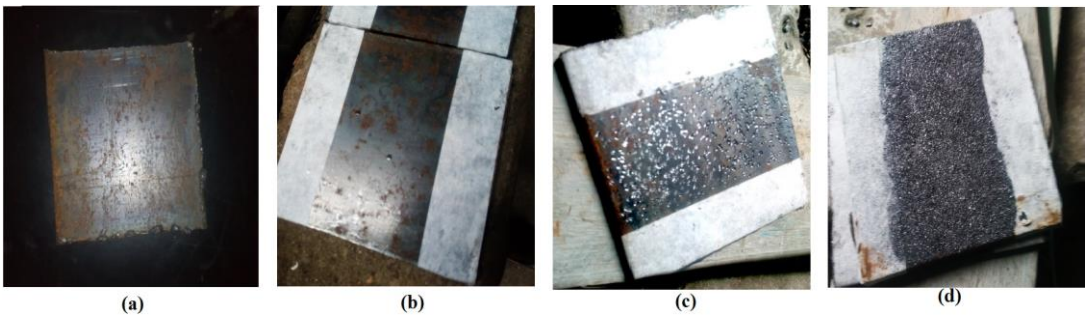

Fig. 1: Representation of the substrate material in its various forms: (a) as-received substrate, (b) degreased and cleaned substrate, (c) mechanically roughened substrate and (d) substrate pre-coated with pasty mass of silicon carbide

GMA melting was adopted for the incorporation of the pre-placed SiC into the substrate under varying process parameters as presented in Table 2. The melting heat delivered to the samples was estimated using Eq. (1), where HI is the heat input ($kJmm^{-1}$), η is the efficiency of the arc melting process, I is the arc current (A), V is the voltage across the terminals (V), and *v* is the electrode transverse speed (mm/sec) (Amuda and Mridha, 2011). Efficiency of GMA melting process was taken as 0.65 with adequate consideration for heat losses (Quintino *et al.*, 2013). Nine pre-placed coatings were melted at different combinations of process parameters listed in Table 2 with the tenth sample representing the control sample. Residual powder from un-melted region of the GMA melted samples were removed and cleaned prior to further characterisation.

Transverse sections of the samples were prepared for microstructural characterisation following procedures provided in Amuda *et al.* (2017). Etching of appropriately polished samples was done in nital solution of 3% nitric acid and 97% methanol for 7 seconds. Macroprofiling was conducted on a zeiss carls stereomicroscope to estimate the width and depth of penetration of the preplaced SiC powder. Further, microstructural characterisations were conducted on a CETI model metallurgical microscope. Microhardness profiles of the polished coating samples were acquired from five positions in both longitudinal and transverse directions using Vickers hardness tester as illustrated in Fig. 2.

Table 2: Matrix of process parameter combinations

Sample No.	**Current (A)**	**Speed (mm/sec)**	**Voltage (V)**	**HI ($KJmm^{-1}$)**
Sample 1	200	5	40	1.04
Sample 2	200	3.33	40	1.56
Sample 3	200	2.5	40	2.08
Sample 4	250	5	40	1.30
Sample 5	250	3.33	40	1.95
Sample 6	250	2.5	40	2.6
Sample 7	300	5	40	1.56
Sample 8	300	3.33	40	2.34
Sample 9	300	2.5	40	3.12
Control Sample	0	0	0	0

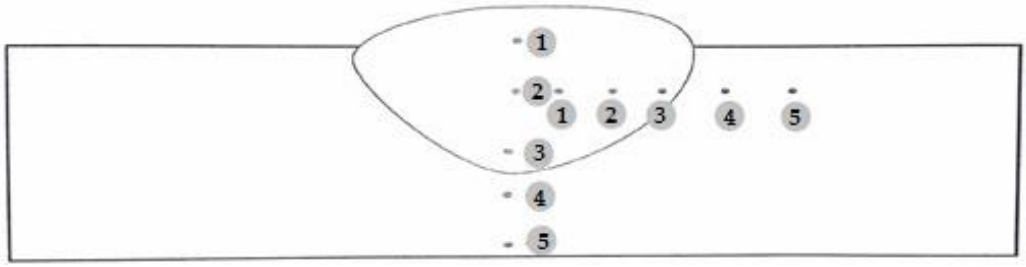

Fig. 2: Indication of microhardness indentation positions in both the longitudinal and transverse directions of the substrate

Wear characterisation was conducted on the coatings using an improvised pin and disk type machine in which a mechanical abrasive was mounted on a

$$HI = \frac{\eta IV}{\upsilon} \quad (1)$$

metallurgical polishing machine. The samples served as the pin while the mechanical abrasive material served as the disk that rotated about its central axis. The characterizations were conducted at two different speeds for three different durations and six different sliding distances provided in Table 3.

Table 3: Matrix of wear test schedule

Speed (rev/sec)	**Time (sec)**	**Sliding Distance (rev)**
125	60	7,500
125	120	15,000
125	180	22,500
250	60	15,000
250	120	30,000
250	180	45,000

The corrosion behaviors of the coatings were evaluated in hydrochloric acid (HCl), sodium hydroxide (NaOH) and sodium chloride (NaCl) solutions using gravimetric technique. The weight loss of the samples immersed in the environments was acquired at intervals of two weeks for three months. Eq. (2) adopted from the investigation of Pierre (2000) was used to derive the corrosion rate for each sample where CR is the corrosion rate (mpy), K is the corrosion constant, D is the desnsity of material(g/cm^3), A is the area of material suceptible to corrosion(cm^2), t is the time of immersion(hr), W is the weight loss of samples.

$$CR = \frac{W * K}{D * A * t} \tag{2}$$

Linear polarization was performed on selected samples with heat input 1.04 kJ/mm, 3.12 kJ/mm and the control sample. The test was conducted on 100 mm x 100 mm polished sample in the range 10 to 15mV using a potentiostat (Model 2000: Toho Technical Research). The test samples were the working electrode, whilst platinum plate was used as the counter electrode. Saturated calomel electrode (SCE) was the reference electrode.

3.0 RESULTS AND DISCUSSION

3.1 Macroprofiling the Resolidified Substrate and Analysis of Degree of Dilution

Visual inspection of the resolidified clads indicates the generation of smooth and defect free surfaces devoid of any porosity across all process parameters. The topography of a representative resolidified clad shown in Fig. 3 reveals ripple marks aligned orthogonal to the welding direction.

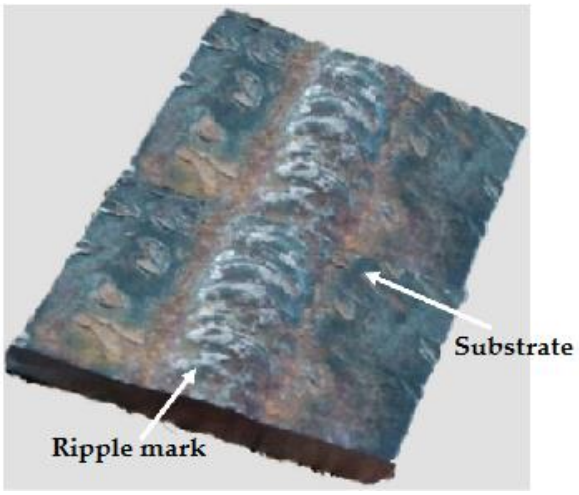

Fig. 3: Topography of a representative arc melted sic modified mild steel

The macroprofile of the resolidified clad showing the cross section in terms of the width and depth of melt track is presented in Fig. 4 for melting conducted at heat input of 1.04, 1.30 and 2.34 kJ/mm, respectively. The degree of dilution in the resolidified clad estimated from the ratio of width to depth is presented in Table 4. The table reveals that the degree of dilution increases with increasing heat input except for the clad produced at a heat input of 3.12 kJ where a reduction was obtained in the degree of dilution. The decrease in the degree of dilution was postulated to be attributed to the low traverse speed at the heat input of 3.12 kJ/mm relative to other melting conditions which enabled the substrate to have a longer interaction time with the melting torch (Awarun, 2018). This leads to more materials being melted in the thickness direction compared to what was obtained at a heat input of 1.04 kJ/mm. The table equally demonstrates that the use of higher arc current results in a wider width while higher traverse speed generates shallow depth in the thickness direction. Higher current delivers more energy to the substrate and hence melts more volume of materials in the surface while the melting speed

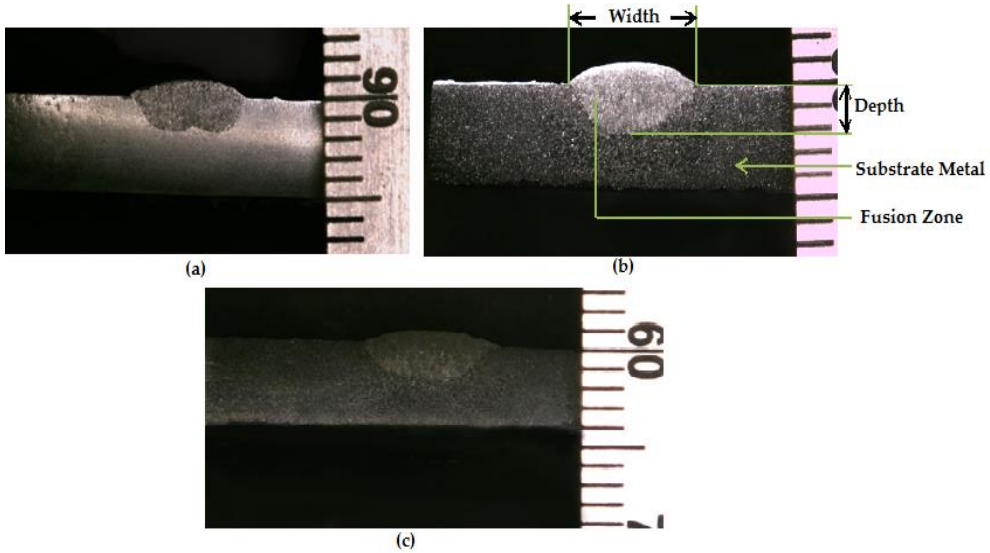

Fig. 4: Macroprofile of resolidified clad showing varying degree of dilution at different heat inputs: (a) 1.04 kJ/mm (b) 1.30 kJ/mm and (c) 2.34 kJ/mm

influences the duration of interaction of the melting torch with the substrate; hence the depth of the resolidified clad. This is in agreement with the work of Daramola (2017) which attributed the wider width of resolidified clad to the adoption of higher threshold of arc current. Therefore, the width of the clad is determined by the arc current while the depth is determined by the traverse speed during melting.

Table 4: Degree of dilution of SiC modified mild steel at varying heat input

Current (A)	Speed (mm/sec)	Heat Input (kJ/mm)	Width (mm)	Depth (mm)	Degree of Dilution
200	5.00	1.04	5.40	2.64	2.05
200	3.33	1.30	7.00	3.15	2.22
200	2.50	1.56	8.00	3.50	2.30
250	5.00	1.562	6.00	2.60	2.31
250	3.33	1.95	7.00	2.70	2.60
250	2.50	2.08	7.80	2.90	2.70
300	5.00	2.34	6.80	2.35	2.90
300	3.33	2.60	7.80	2.55	3.06
300	2.50	3.12	8.00	3.20	2.50

3.2 Microstructural Analysis

The microstructure of the as-received substrate shown in Fig. 5 consists of coarse-grained ferrite networked by iron carbide. However, the microstructure of the resolidified clad shown in Fig. 6 reveal the formation of needle- like dendritic structure which grows in the direction of the melting torch. The dendritic structure observed in the coated layer could be attributed to the rapid solidification consequent upon the removal of the melting torch. The morphology of the structure showed preferred growth direction along energetically favourable crystallographic directions (Dantzig and Rappaz, 2009). The presence of similar microstructure in related surface modification researches accomplished via other arc melting processes has been reported in literature (Buytoz, 2006; Woldan *et al.*, 2003). The evolving microstructures at other heat inputs are shown in Fig. 7. These microstructures exhibit growing columnar grains in relation to the increasing heat input deliver to the substrate.

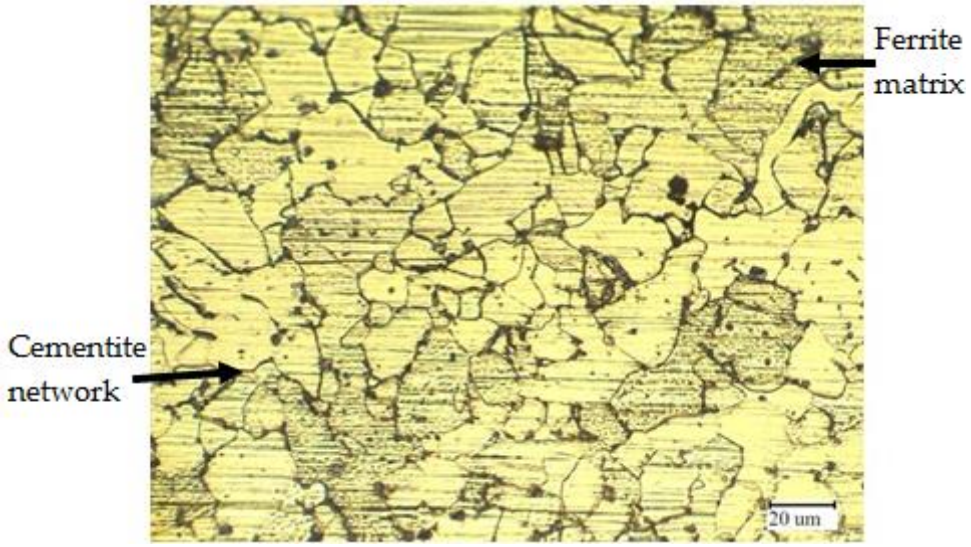

Fig. 5: Microstructure of as-received mild steel substrate

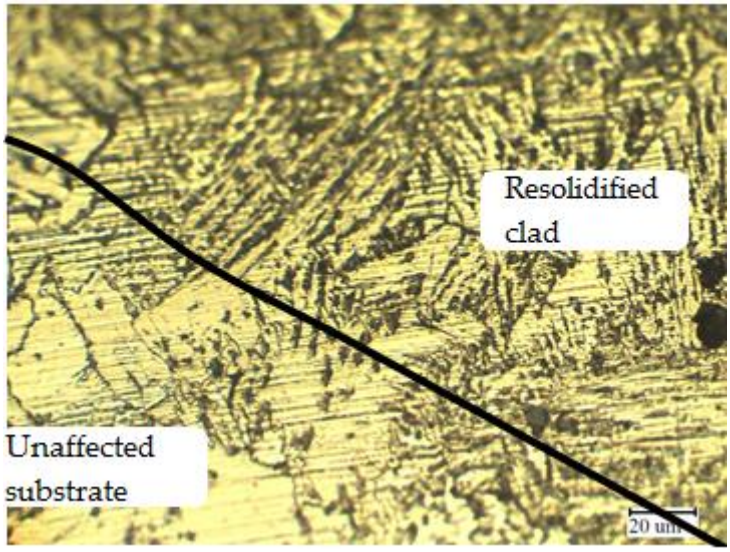

Fig. 6: Microstructure of resolidified clad of sic on mild steel substrate produced at heat input of 1.04 kJ/mm

3.3 Microhardness Profile in Resolidified SiC modified Mild Steel

The hardness profile in the resolidified clad measured along both longitudinal and transverse directions as earlier illustrated in Fig. 2 are shown in Fig. 8. The figure reveals that the hardness values in the resolidified clad in both directions are influenced by the heat input. The hardness value decreases in resolidified clad across the width from the resolidified zone through the heat

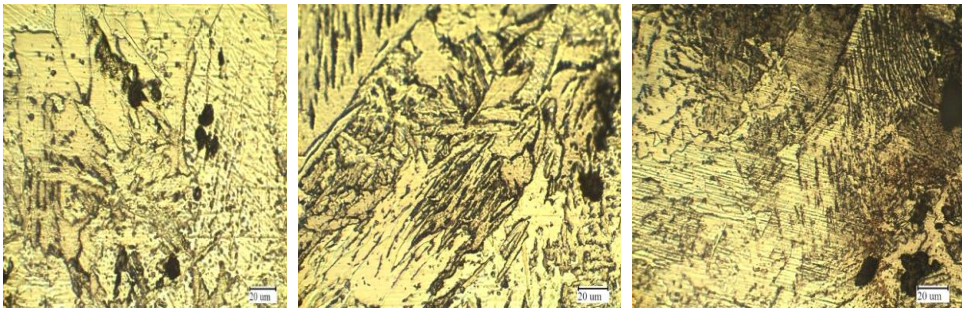

(a) (b) (c)

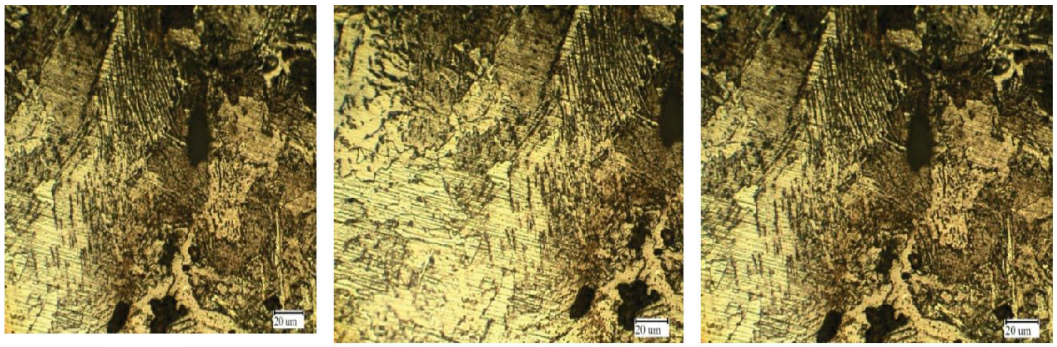

Fig. 7: Microstructure of resolidified clad of sic on mild steel substrate at different heat inputs: (a) 1.30 kJ/mm (b) 1.56 kJ/mm (c) 2.08 kJ/mm (d) 2.34 kJ/mm (e) 2.60 kJ/mm and (f) 3.12 kJ/mm

affected zone to the unaffected substrate material for the clad produced at heat input of 1.04 kJ/mm while the value increases with heat input above 1.30 kJ/mm. A peak hardness value of 200 HV was reached at about 3 mm distance from the surface. The value converges to 100 HV subsequently irrespective of the heat input (see Fig. 8a). The trend is similar in the transverse direction except that the peak value is obtained between 2 mm and 3 mm in the thickness direction (see Fig. 8b). The hardness value decreases towards the melt depth away from the resolidified melt in the transverse direction. The value converges to about 100 HV at further distance beyond 3 mm in the thickness direction. The trend of hardness profiles in Fig. 8 suggests that the region of the substrate affected by the incorporation of SiC is restricted to within 3 mm radius in both the longitudinal and transverse directions. This trend aligns with the macroprofile shown in Fig. 4.

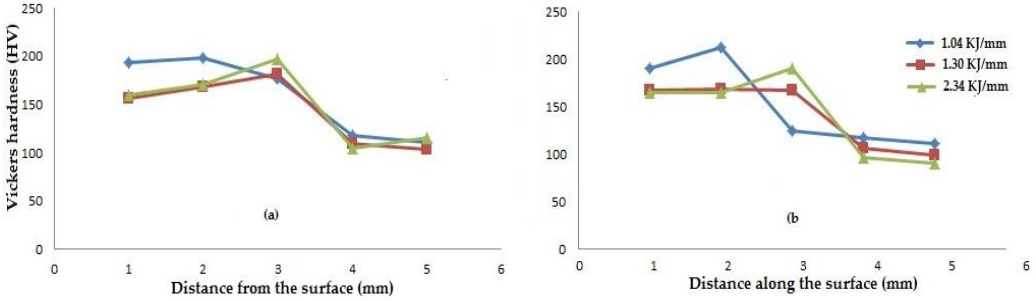

Fig. 8: Vickers hardness profiles of SiC modified mild steel at different heat inputs: (a) longitudinal and (b) transverse directions

3.4 Analysis of Wear in Resolidified Layers

The influence of heat input on the wear behavior of the resolidified clad under different loading conditions is shown in Fig. 9. The figure reveals that SiC modified substrates irrespective of the heat input exhibit reduced wear rate compared to the substrate. The wear rate in uncoated substrate is in the range (0.75 – 1.08) x $10^{-8}mm^3$ whereas the rates in SiC modified substrates are in the range (0.5- 0.8) x $10^{-8}mm^3$, (0.3 – 0.4) x $10^{-8}mm^3$ and (0.1-0.3) x $10^{-8}mm^3$ for heat input of

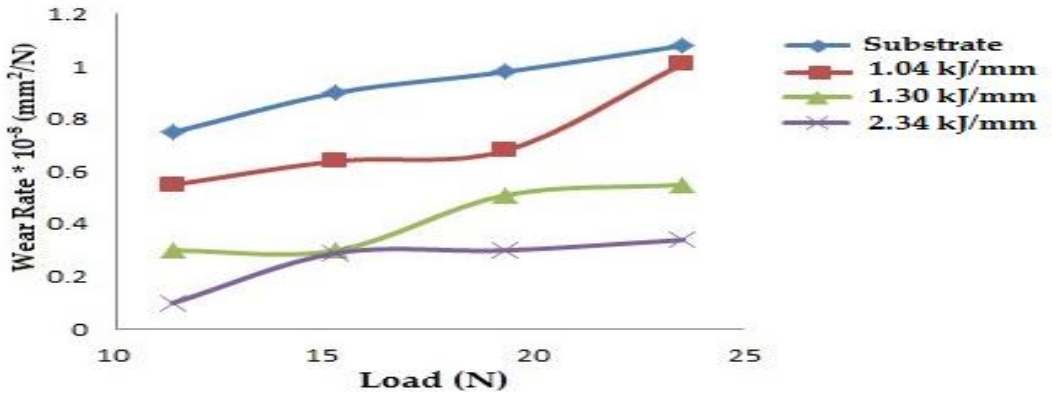

Fig. 9: Influence of applied load on the wear rate of resolidified clad layer at different heat inputs

1.04 kJ/mm, 1.30kJ/mm and 2.34 kJ/mm, respectively. The resolidified clad layer produced at heat input of 2. 34 kJ/mm presents the least wear rate indicating superior wear characteristics. It is presumed that the improved wear characteristic obtained at heat input of 2. 34 kJ/mm is due to the greater dissolution of the

preplaced SiC in the resolidified clad layer which enabled the generation of higher hardness in the resolidified clad layer.

3.5 Analysis of Corrosion Characteristics of the Resolidified Layer

The corrosion behaviour of the resolidified clad layers in the three media of HCl, NaOH and NaCl characterized in terms of corrosion rate is presented in Fig. 10. The figure shows that the resolidified clad layer exhibit better corrosion behaviour than the substrate material in the three media. However, corrosion of the samples is greatest in HCl, followed by NaCl and least in NaOH. The corrosion rates of resolidified clad layers in HCl environment are 63.49 mpy, 56.17

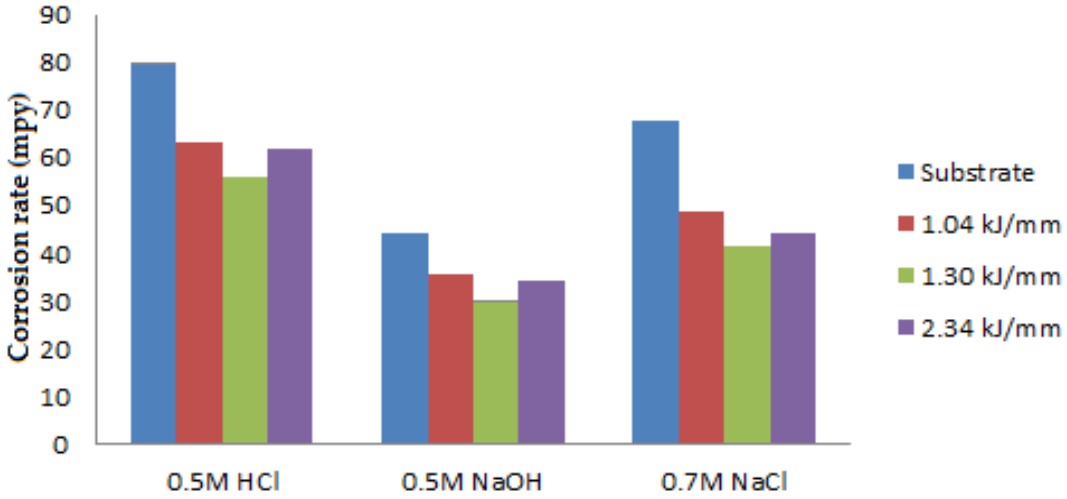

Fig. 10: Corrosion rate of sic modified mild steel in acidic, basic and salt environments

mpy and 62.03 mpy for heat input of 1. 04 kJ/mm, 1.30 kJ/mm and 2.34 kJ/mm, respectively. For NaCl environment, the rates are 48.84 mpy, 41.51 mpy, and 44.44 mpy while in NaOH, they are 35.65 mpy, 29.79 mpy, and 34.19 mpy , respectively. Resolidified clad layers produced at the heat input of 1.304 kJ/mm exhibited the least corrosion rate indicating improved corrosion resistance. The improvement in corrosion resistance obtained in resolidified clad layers relative to the substrate was attributed to the homogenous dendritic structure in the resolidified layers unlike the duplex structure of cementite and ferrite in the substrate.

The linear polarization curves for the resolidified clad layers produced at heat input of 1.04 and 3. 12 kJ/mm in relation to the substrate are shown Fig. 11. The

resolidified clad layers present lower current density and a more negative corrosion potential than the as-received substrate. It is clear from the curves that the electrochemical behaviour of the samples during polarisation aligns with the trend observed in gravimetric analysis.

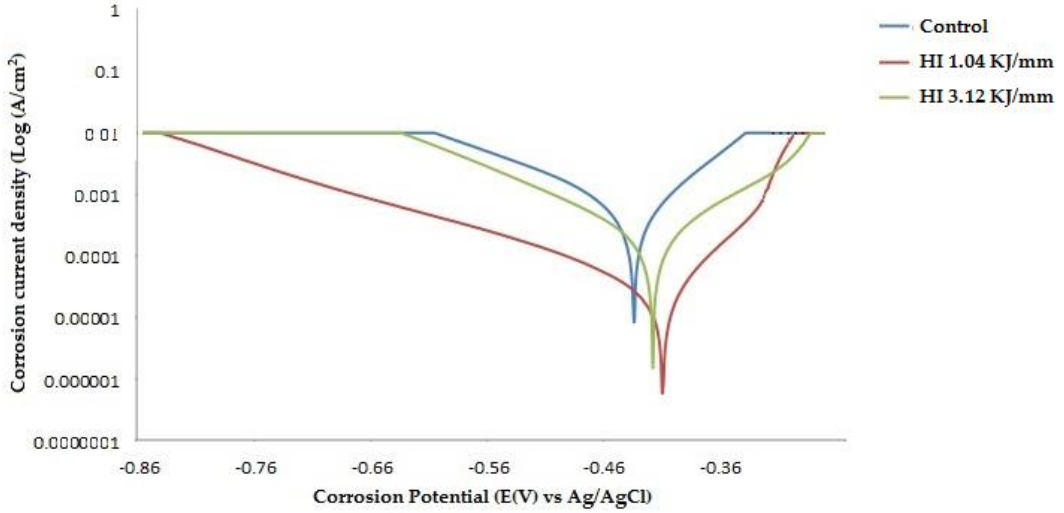

Fig. 11: Polarisation curves in resolidified clad layer melted at heat input of 1.04 kJ/mm and 3.12 kJ/mm

CONCLUSION

The wear and corrosion characteristics of resolidified mild steel substrate modified by the incorporation of SiC into the melt pool using GMA melting technique has been studied. It was established that the geometry of the resolidified layer was influenced by a composite of the arc current and the electrode traverse speed in the form of heat input. The width of the resolidified zone was affected by the arc current while the depth was dependent on the electrode traverse speed. The degree of dilution in the resolidified clad layer increases with increasing heat input peaking at 3.06 at heat input of 2.60 kJ/mm. The study equally established that lower current and higher electrode traverse speed minimizes the degree of dilution suggesting minimal melting of the substrate material. The resolidified clad layer exhibited higher hardness than the substrate in both the longitudinal and transverse directions irrespective of the melting process parameters.

The improvement obtained in the wear behaviour of the surface modified substrate was attributed to its higher hardness which was influenced by the formation of SiC reinforced dendritic structure in the substrate. Similarly, the corrosion behaviour of the surface modified substrate improved across the three

media considered. In each of these media, the improvement in corrosion rate peaked at 29%, 33% and 35% in 0.5MHCl, 0.5MNaOH and 0.7MNaCl, respectively, at heat input of about 1.3 kJ/mm. This heat input corresponds to a melting current of 250 A and electrode traverse speed of 5 mm/sec. The improvement obtained in both the wear and corrosion resistances of the surface modified mild steel suggests that low-cost gas metal arc melting technique which is conventionally used for welding can be readily adapted for surface modification as an alternative to the capital intensive laser melting technique.

ACKNOWLEDGEMENT

The authors appreciate the Management of Midwal Engineering Services Limited, Lekki, Lagos, Nigeria for permitting the use of their facilities for both microhardness and microstructural characterisations.

REFERENCES

Abbas, G. and Ghazanfar, U. (2005). Two body abrasive wear studies of laser produced stainless steel and stainless steel + SiC composite clads. *Wear.* 258 (1-4): 258–264.

Amuda, M.O.H. and Mridha, S. (2011). Effect of energy input on microstructure and hardness of TIG welded AISI 430-ferritic stainless steel. *Adv. Mater. Res*. 264: 390-396.

Amuda, M. O. H., Lawal, T.F., Enumah, K.S., Ezeonu, L.L and Onitiri, M. A. (2017). Influence of thermal treatments on sensitization in Cr-Mn-Cu austenitic stainless steel welds, *In press, UNILAG J. Med. Sci. Technol.* 1-15.

Awarun, A. B. (2018). Wear characteristics of graphite coated mild steel, B.Sc. Metallurgical and Materials Engineering Final Year Project, Department of Metallurgical and Materials Engineering, University of Lagos, Nigeria. 73p.

Buytoz, S. (2006). Microstructural properties of SiC based hardfacing on low alloy steel. *Surf. Coat. Technol.* 200: 3734– 3742.

Dantzig, J.A. and Rappaz, M. (2009). Solidification. EPFL Press, Lausanne, Switzerland. 305p.

Darabara, M., Bourithis, L., Diplas, S. and Papadimitriou, G.D. (2012). Corrosion and wear properties of composite coatings reinforced with TiB_2 particles produced by PTA on steel substrate in different atmospheres. *Int. Sch. Res. Net –Corros.* 2012 (898650): 1-9.

Daramola, O. (2016). Wear and corrosion characteristics of silicon carbide surface modified mild steel. B.Sc. Metallurgical and Materials Engineering Final Year Project, Department of Metallurgical and Materials Engineering, University of Lagos, Nigeria. 54p.

Dyuti, S., Mridha, S. and Shaha, S. K. (2011). Wear behavior of modified surface layer produced by TIG melting of preplaced Ti powder in nitrogen environment. *Adv. Mater. Res.* 264-265: 1427-1432.

Edenhofer, B., Joritz, D., Rink, M. and Voges, K. (2015). Carburizing of steels, Part Three In: Mittemeijer, E.J. and Somers, M.A.J. (Eds.) *Thermochemical Surface Engineering of Steels-Improving Materials Performance*. Woodhead Publishing, Cambridge, pp. 485-553.

Grum, J. and Znidaršič, M. (2008). Laser refining of a surface layer with silicon carbide. *Mater. Manuf. Processes.* 23 (2):215-219.

Harish, R.G., Sanjivi, A. and Sellamuthu, R. (2014). Improving surface hardness of mild steel plates by addition of silicon carbide using gas tungsten arc as heat source. *Appl. Mech. Mater.* 592-594: 879-882.

Krastev, D. (2012). Improvement of corrosion resistance of steels by surface modification. Corrosion Resistance. Shih (Ed.) 295-317

Lathabai S. (2011). Joining of aluminium and its alloys. *Fundamentals of Aluminium Metallurgy. Production, Processing and Applications*. Woodhead Publishing Series in Metals and Surface Engineering, Cambridge, pp. 607-654.

Majumdar, J.D. (2010). Development of in-situ composite surface on mild steel by laser surface alloying with silicon and its remelting. *Surf. Coat. Technol.* 205(7): 1820-1825.

Majumdar, J. D., Ramesh, C. B., Nath, A.K. and Manna, I. (2008). Studies on compositionally graded silicon carbide dispersed composite surface on mild steel developed by laser surface cladding. *J. Mater. Process. Technol.* 203:505–512.

Majumder, J. D. (2017). Laser-aided direct metal deposition of metals and alloys. *Laser Additive Manufacturing*, Woodhead Publishing Series in Electronic and Optical Materials, Cambridge, pp. 21-53.

Mohd, T.A.L., Nagentrau, M., Kamdi, Z., Ismail, M. I. and Omar, A. S. (2018). Effects of weldment layer on the tungsten carbide hardfacing microstructure. *IOP Conf. Series, Mater. Sci. Eng.* 295.

Munawar, I., Shaukat, I., Arshad, M., Kaleem, A. and Anwar, H. (2010). Surface modification of mild steel with boron carbide reinforcement by electron beam melting. *Vacuum*. 85(1):45-47.

Muñoz-Escalona, P., Mridha, S. and Baker, T. N. (2016). Effect of silicon carbide particle size on microstructure and properties of a coating layer on steel produced by TIG technique. *Adv. Mater. Process. Technol.* 2(4):451-460.

Quintino, L. (2014). Overview of coating technologies. *Surface Modification by Solid State Processing*. Woodhead Publishing, Cambridge, pp.1-24

Quintino, L., Liskevich, O., Vilarinho, L. and Scotti, A. (2013). Heat input in full penetration welds in gas metal arc welding (GMAW). *Int. J. Adv. Manuf. Technol.* 862-870.

Roman, T.S., Matjaz, N.Z. and Janez, G. (2013). Crack-growth behavior of laser surface-alloyed low-carbon steel. *J. Mater. Eng. Perform*, 22:2542–2549

Schneider, M.J. and Chatterjee, M.S. (2013). Introduction to surface hardening of steels. In: *Steel Heat Treating Fundamentals and Processes*. ASM Handbook. 4A:389-398.

Wahab, Q., Willander, M. and Friesel, M. (2006). Silicon carbide and diamond for high temperature device applications. *J. Mater. Sci. – Mater. Electron.* 17: 1.

Weman, K. (2012). MIG/MAG welding. *Welding Processes Handbook* (Second Edition).Woodhead Publishing Series in Welding and Other Joining Technologies, Cambridge, pp. 75-97.

Woldan, A., Kusi´nski, J. and Tasak, E. (2003). The microstructure of plain carbon steel laser-alloyed with silicon carbide. *Mater. Chem. Phys.* 81:507–509.